Cancer Immunology, Immunotherapy (2023) 72:1685–1698
https://doi.org/10.1007/s00262-022-03358-3

RESEARCH

Interaction of glioma-associated microglia/macrophages and anti-PD1 immunotherapy

Chunhua Wang[1,2,3] · Quan Chen[1,3] · Meiqing Chen[1,2] · Sizhen Guo[1] · Ping Hou[1] · Yulian Zou[1] · Jun Wang[1] · Bailin He[1] · Qiuyu Zhang[1] · Lieping Chen[1,4] · Liqun Luo[1]

Received: 25 October 2022 / Accepted: 23 December 2022 / Published online: 9 January 2023

Abstract

Anti-PD-1-based therapy has resulted in a minimal clinical response in malignant gliomas. Gliomas contain numerous glioma-associated microglia/macrophages (GAMs), reported to contribute to an immunosuppressive microenvironment and promote glioma progression. However, whether and how GAMs affect anti-PD-1 immunotherapy in glioma remains unclear. Here, we demonstrated that M1-like GAMs contribute to the anti-PD-1 therapeutic response, while the accumulation of M2-like GAMs is associated with therapeutic resistance. Furthermore, we found that PD-L1 ablation reverses GAMs M2-like phenotype and is beneficial to anti-PD-1 therapy. We also demonstrated that tumor-induced impairment of the antigen-presenting function of GAMs could limit the antitumor immunity of $CD4^+$ T cells in anti-PD-1 therapy. Our study highlights the impact of GAMs activation on anti-PD-1 treatment and provides new insights into the role of GAMs in regulating anti-PD-1 therapy in gliomas.

Keywords Glioma · Glioma-associated microglia/macrophages · Immunotherapy · PD-1 (programmed death-1) · PD-L1 (programmed death-ligand 1) · $CD4^+$ T cells

Abbreviations

APCs	Antigen-presenting cells
Arg1	Arginase 1
DAPI	4′, 6-Diamidino-2-phenylindole
DMEM	Dulbecco's modified Eagle's medium
FACS	Fluorescence-activated cell sorting
GAMs	Glioma-associated microglia/macrophages
GBM	Glioblastoma
IFN-γ	Interferon-γ
iNOS	Inducible nitric oxide synthase
MCP-1	Monocyte chemoattractant protein-1
MHC-II	Major histocompatibility complex class II
OVA	Ovalbumin
PD-1	Programmed cell death protein 1
PD-L1	Programmed death-ligand 1
TME	Tumor microenvironment
TGF-β	Transforming growth factor-beta
TNF-α	Tumor necrosis factor α

Chunhua Wang and Quan Chen have contributed equally.

✉ Liqun Luo
liqunluo@hotmail.com

1 Institute of Immunotherapy, Fujian Medical University, No. 1, Xuefu North Road, Minhou County, Fuzhou 350122, Fujian, People's Republic of China

2 Department of Pharmacology, School of Pharmacy, Fujian Medical University, No. 1, Xuefu North Road, Minhou County, Fuzhou 350122, Fujian, People's Republic of China

3 Department of Neurosurgery, Fujian Medical University Union Hospital, No. 29, Xinquan Road, Fuzhou 350001, Fujian, People's Republic of China

4 Department of Immunobiology, Yale University West Campus, MIC331, 600 West Campus Drive, West Haven, CT 06516, USA

Introduction

Malignant gliomas are the most common and lethal primary brain tumors, with limited treatment options and poor survival rates. Despite the aggressive use of surgery, radiotherapy, and chemotherapy, the 5-year survival rate for glioma is approximately 30%, and for those with glioblastoma (GBM), it is even lower at 7% [1].

Immunotherapy, especially anti-programmed cell death protein 1/programmed death-ligand 1 (anti-PD-1/PD-L1) therapy, acts primarily on correcting a dysfunctional immune response locally within the tumor microenvironment (TME)

and leads to reinvigorating T cell antitumor responses and tumor rejection [2]. Anti-PD-1/PD-L1 therapy improved patient survival in many advanced malignancies, but no breakthrough in GBM [3–6]. A phase III clinical trial (Checkmate 143) demonstrated that nivolumab, which targets PD-1, did not produce survival benefits compared with bevacizumab in recurrent GBM patients, and only 7.8% of patients showed objective responses [4]. The underlying mechanisms of glioma resistance to anti-PD-1therapy are not fully clear. As the key effector cells of anti-PD-1 therapy, T cells have been characterized by their poor infiltration and uniquely severe exhaustion signature in GBM, which may be regulated by the immunosuppressive TME [7–9].

Glioma-associated microglia/macrophages (GAMs) are the most abundant immune cells, constituting up to 30–50% of the bulk glioma cells [10, 11]. They are generally divided into the proinflammatory M1 phenotype and anti-inflammatory M2 phenotype, but it is noteworthy that their activation is a highly dynamic process and can polarize or interconvert under various regulatory factors [12, 13]. M1-like GAMs are often associated with the expression of major histocompatibility complex class II (MHC-II), CD80, CD86, CD40, and inducible nitric oxide synthase (iNOS), whereas CD206, arginase 1 (Arg1), PD-1, and PD-L1 are associated with more M2-like GAMs [14–17].

GAMs are usually activated into M2-like phenotypes as key drivers of the local immunosuppressive microenvironment [18–20]. GAMs can directly mediate the anergy, exhaustion, and apoptosis of lymphocytes by expressing PD-L1 and FasL and secreting immunosuppressive cytokines such as transforming growth factor-beta (TGF-β), interleukin (IL)-10, and IL-6, which weaken antitumor immunity and promote tumor immune escape [19, 21]. A recent study has shown that a higher density of $CD68^{+}HLA\text{-}DR^{-}$ macrophages were observed in PTEN-mutated glioblastoma, while enrichment of PTEN mutations was associated with non-response to anti-PD-1 therapy [22].

On the other hand, microglia and macrophages are also essential phagocytes and antigen-presenting cells (APCs) in the glioma microenvironment, which can modulate innate and adaptive immune responses necessary for tumor eradication/suppression [23, 24]. In particular, MHC-II-restricted antigen presentation is essential for $CD4^{+}$ T cell-mediated antitumor immunity, which is required for responses to anti-PD-1/PD-L1 immunotherapy [25, 26].

Given the crucial role of GAMs as immune modulators in glioma, an in-depth understanding of the activation and function of GAMs in the context of anti-PD-1 treatment is essential to reveal the underlying mechanisms of immunotherapy resistance in glioma. Here, we demonstrate that activation of M1-like GAMs is necessary for responding to anti-PD-1 therapy, while accumulation of M2-like GAMs is responsible for therapy resistance. Furthermore, we found that GAMs-derived PD-L1 inhibited the M1-like activation of GAMs and weakened anti-PD-1 therapy. We also investigated the potential effect of GAMs on $CD4^{+}$ T cell-mediated antitumor immunity in anti-PD-1 therapy.

Materials and methods

Animals and cell lines

Male C57BL/6J mice, aged 6–8 weeks, were purchased from Beijing Vital River Laboratory Animal Technology Co., Ltd. (Beijing, China). PD-L1-deficient ($PD\text{-}L1^{-/-}$) mice on the C57BL/6 background were bred in-house [27]. OT-II transgenic mice were purchased from the Model Animal Research Center of Nanjing University (Nanjing, China). All the mice were housed under pathogen-free conditions at the Laboratory Animal Center of Fujian Medical University (Fuzhou, China).

The glioma cell line GL261-Luc was obtained from Dr. Lie-Ping Chen (Yale University). The murine microglial cell line BV2 was purchased from the China Center for Type Culture Collection (CCTCC, Wuhan, China). The cell lines were cultured in Dulbecco's modified Eagle's medium (DMEM) supplemented with 10% fetal bovine serum (FBS) and 1% penicillin–streptomycin. The tumor-conditioned medium was collected after 24 h from 80% confluent GL261-Luc cultures and filtered through a 0.22-μm filter. All cell lines were tested using a PCR mycoplasma test kit (HuaAn Biotechnologies, China) to ensure that the cells were free of mycoplasma contamination and were reliable for experiments.

Tumor model and treatment

Male wild-type (WT) or $PD\text{-}L1^{-/-}$ C57BL/6J mice (6–8 weeks old) were used for orthotopic glioma experiments. Briefly, anesthetized mice were immobilized and mounted on a stereotactic head holder in a flat skull position. GL261-Luc cells (1×10^5) were stereotactically injected in a 4 μL volume into the right striatum at 2 min following coordinates: 2 mm lateral from bregma and 2.5 mm deep from the cortical surface. The needle was slowly removed from the injection canal, the bone pore was sealed with bone wax, and the skin was sutured. The mice whose tumors were too small (radiance $< 10^5$ p/s/cm/sr) or too large (radiance $> 10^8$ p/s/cm/sr) on day 6 after tumor inoculation were excluded. Tumor-bearing mice were randomized into groups by random figure table. The tumor size was measured by bioluminescence, and the survival time of mice was observed. The mice were euthanized when they showed predetermined signs

of neurological deficits (failure to ambulate, weight loss > 30% body mass, lethargy, hunched posture) or the experiment was completed.

For anti-PD-1 treatment, mice were intraperitoneally injected with anti-PD-1 antibodies (clone G4) at a dose of 10 mg/kg from day 7, 10, or 16 after tumor inoculation. The same follow-up dose of antibodies was administered three days later.

For GAMs depletion, clodronate liposomes were stereotactically injected into the tumor in a 10 μL volume. The control group received PBS control liposomes at the same volume.

For $CD4^+$ T cell depletion, mice were intraperitoneally injected with 500 μg anti-CD4 antibodies (clone GK1.5) on day 7 after tumor inoculation. The same follow-up dose of antibodies was administered three days later.

In vivo bioluminescent imaging

In vivo bioluminescence imaging was performed in the tumor-bearing mice. Before imaging, mice were intraperitoneally injected with 200 μL of 15 mg/mL D-luciferin (Perkin-Elmer, USA) and left for 10 min. Luminescence was detected using IVIS Spectrum (Perkin-Elmer, USA), and image analysis was performed using Living Image Software (Perkin-Elmer, USA).

Fluorescence-activated cell sorting (FACS) analysis

For cell preparation, mice were euthanized using carbon dioxide, and transcardial perfusion was performed with chilled PBS for 3 min to remove blood, followed by dissection of the brain. Tumor-bearing hemispheres were dissociated into single cells using a gentleMACS Octo Dissociator (Miltenyi Biotec, Germany) and solutions provided with the Adult Brain Dissociation Kit (Miltenyi Biotec, Germany) according to the manufacturer's instructions. The dissociated tissues were filtered using 70-μm strainers, and debris and contaminating erythrocytes were removed. For immunofluorescence staining, the cells were preincubated with anti-CD16/CD32 (clone 2.4G2) for 20 min, followed by 30-min incubation with conjugated antibodies for extracellular markers. Intracellular antigens were detected using an intracellular fixation and permeabilization buffer set (eBiosciences). All the antibodies used in these experiments are listed in Supplemental Table 1. Proper isotype and compensation controls were performed in parallel. Cells were analyzed using a FACSVerse flow cytometer (BD Biosciences, USA), and data were processed using FlowJo software (Tree Star, USA).

Immunohistochemistry and immunofluorescence

The tissues were fixed in 4% paraformaldehyde for 24 h, embedded in paraffin, and sectioned serially (3 μm). For immunohistochemical staining, the slides were deparaffinized and subjected to graded rehydration. After antigen retrieval (citrate buffer, pH 6.0) and blocking with goat serum, the slides were incubated with primary antibodies at a dilution of 1:2000 for Iba1 (Abcam, USA) overnight. The primary antibodies were detected using a rabbit-enhanced polymer detection system (PV9001, Zhongshan Golden Bridge Biotechnology, China) with a polyclonal horseradish peroxidase-conjugated secondary antibody and 3,3′-diaminobenzidine substrate. For immunofluorescence staining, the tissue sections were blocked with goat serum following heat-induced antigen retrieval. Primary antibodies were then incubated at a dilution of 1:100 for Iba1 or CD4, CD8, and PD-L1 overnight. The secondary antibodies conjugated to Alexa Fluor 488, 568, and 647 were incubated with the slides at 1:200 dilution for 2 h at room temperature, and 4′,6-diamidino-2-phenylindole (DAPI, Sigma-Aldrich, USA) was used as a nuclear counterstain. All images were taken using the EVOS™ FL Auto Imaging system (Thermo Fisher) and analyzed using Image J software.

Microglia isolation and cultivation

Microglia were isolated from 6- to 8-week-old C57BL/6 mice brains using an Adult Brain Dissociation Kit (Miltenyi Biotec, Germany) and magnetic CD11b microbeads (Miltenyi Biotec, Germany). Briefly, the cerebrum was removed and cut into small pieces. The tissue was dissociated via enzymatic digestion using a gentleMACS Octo Dissociator (Miltenyi Biotec, Germany). The cell suspension was filtered through a 70 μM cell strainer, and debris and red blood cells were removed. The desired cells were labeled with CD11b MicroBeads for 20 min, washed with PBS, and magnetically separated. Labeled CD11b-positive cells (microglia) were enriched and harvested for purity checks and further tests.

To cultivate microglia, isolated microglia were seeded into 48-well plates at a density of 1×10^5 cells per well in 100 μL DMEM medium containing 10% FBS (Gibco, USA), 1% penicillin/streptomycin (Gibco, USA), 5 ng/mL recombinant TGF-β1 (PeproTech, USA), and 10 ng/mL recombinant mouse macrophage colony-stimulating factor (M-CSF, PeproTech, USA). Half of the medium was changed every three days for seven days before further treatment.

Naïve $CD4^+$ T cell isolation and co-culture assay

The EasySep™ Mouse Naïve CD4 T Cell Isolation Kit (Stemcell Technologies Inc., Canada) was used to purify naïve $CD4^+$ T cells ($CD4^+CD44^{low}CD62L^{high}$) from the

spleens of OT-II mice according to the manufacturer's instructions. For T cell co-culture assays, primary microglia were pretreated with 50% tumor-conditioned medium or complete DMEM supplemented with 50 μg/mL ovalbumin (OVA) 323–339 peptide (GenScript, China) for 24 h. Then, the microglia were washed with PBS and co-cultured with naïve CD4 T cells labeled with CFSE at a ratio of 2:1. After three days of co-culture, both microglia and T cells were analyzed using FACS, and the supernatant was collected for cytokine detection.

Cytokines analysis by cytometric bead array

Cytokine levels in the supernatant of co-cultured cells were measured using a cytometric bead array Mouse Inflammation Kit (BD Biosciences, USA). The kit was used according to the manufacturer's instructions to measure the levels of mouse IL-6, monocyte chemoattractant protein-1 (MCP-1), interferon-γ (IFN-γ), tumor necrosis factor α (TNF-α), IL-12p70, and anti-inflammatory cytokine IL-10 in a single sample. Briefly, mouse inflammation standards were prepared with 2 mL of assay diluent, and six mouse inflammation capture beads were mixed thoroughly. Next, 50 μL of mixed capture beads was incubated with the same volume of each mouse inflammation standard dilution or each sample. Then, 50 μL of mouse inflammation PE detection reagent was added to all assay tubes and incubated for 2 h at room temperature, protected from light. After washing with washing buffer, the samples were measured using a FACSVerse flow cytometer (BD Biosciences), and the data were analyzed using FCAP Array version 3.0.1.

Statistics

Statistical analyses were performed using Prism 9 software (GraphPad, Canada). All data were shown as the mean ± SD unless otherwise stated, and significant differences were determined using a two-tailed Student's *t* test or one-way ANOVA with Tukey's multiple comparison test. Kaplan–Meier survival curves were analyzed with a log-rank test. *P* values < 0.05 were considered significant (*$P < 0.05$, **$P < 0.01$, ***$P < 0.001$).

Results

GAMs are dominant immune cells accumulated during the glioma progression

To evaluate the role of GAMs in glioma progression and the TME molded, we assessed the kinetics of GAMs infiltration and activation in glioma generated by intraceregral inoculation of GL261-Luc glioma cells in C57BL/6J mice. We found that the majorities of immune cells infiltrating the tumors were GAMs (Fig. 1a–c). In particular, $CD8^+$ T cells, but not $CD4^+$ T cells, rarely invade the core of the tumor (Fig. 1b). Meanwhile, the expressions of CD206, PD-1, and PD-L1 on GAMs continued to increase during tumor progression. In addition, MHC-II expression also increased in the early stage of tumor progression but slightly decreased in the late stage (Fig. 1d). These data indicate that GAMs are the dominant immune cells that dynamically shift to M2-like immunosuppressive phenotypes with glioma progression.

Accumulation of GAMs with M2-like phenotype accompanies resistance to anti-PD-1 therapy

So far, no obvious clinical benefit was substantiated in a randomized phase III clinical trial evaluating an anti-PD-1 antibody therapy for recurrent glioblastoma [4]. Indeed, no therapeutic effect was observed in intracerebral transplanted GL261-Luc tumors treated with anti-PD-1 antibody treatment on days 16 after tumor inoculation. However, anti-PD-1 therapy led to 83.3% and 50% tumor regression and long-term survival in mice when the treatment began on days 7 and 10, respectively (Fig. 2a–d). To investigate the effect of GAMs on anti-PD-1 antibody therapy, we compared the infiltration and activation of GAMs on days 7 and 16 when the tumors were sensitive or resistant to anti-PD-1 therapy. FACS analysis revealed that GAMs significantly increased in number and expressed more Arg1, PD-1, and PD-L1 on day 16 than on day 7 after tumor inoculation. (Fig. 2e). These data suggest the correlation between the M2-like transition of GAMs and resistance to anti-PD-1 therapy.

GAMs depletion impaired the antitumor efficacy of anti-PD-1 therapy

To confirm the role of GAMs in anti-PD-1 therapy, we attempted to deplete GAMs via intratumoral injection of clodronate liposomes (Fig. 3a). The results showed that clodrosome treatment significantly decreased $F4/80^+$ GAMs (Fig. 3b), but did not reduce tumor growth or prolong the survival time of mice (Fig. 3c–e). Furthermore, GAMs depletion weakened the efficacy of anti-PD-1 therapy, with reduced survival (33.3% vs. 50%) and shortened median survival (36 vs. 68.5 days) (Fig. 3c–e). These data suggest that GAMs may partially mediate the antitumor efficacy of anti-PD-1 therapy.

Anti-PD-1 antibody treatment promotes T cells infiltration and GAMs M1-like activation

To determine the potential mechanisms of anti-PD-1 therapy in gliomas, we analyzed the infiltration and activation of T lymphocytes and GAMs after anti-PD-1 treatment.

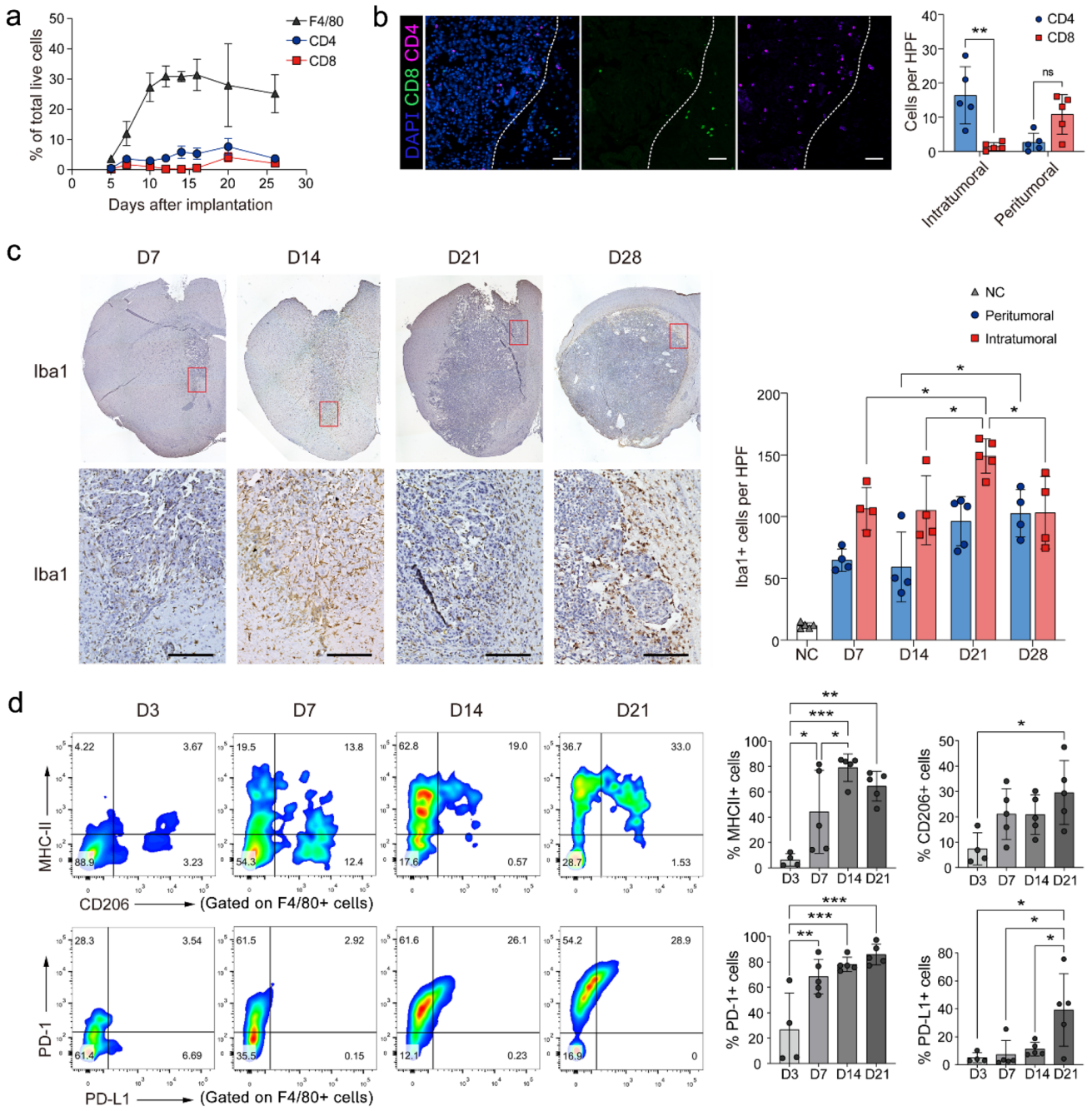

Fig.1 GAMs are dominant tumor-infiltrating immune cells in the glioma progression. **a** The line graph shows the dynamic changes of F4/80$^+$ GAMs, CD4$^+$, and CD8$^+$ T cells in glioma progression, as accessed by FACS. **b** Representative immunofluorescence staining images for CD8$^+$ T cells (green), CD4$^+$ T cells (pink), and DAPI (blue) in the tumor area (scale: 100 μm). The average number of CD8$^+$ and CD4$^+$ T cells in each HPF (400×) was calculated in the right figure ($n=5$). Each mouse was counted from 3 to 5 random HPF. **c** The representative IHC images for Iba1$^+$ cells in the tumor area on days 7, 14, 21, and 28 after tumor inoculation (scale: 100 μm). The statistical analysis results are shown in the right panel. Ctrl: contralateral brain, Peritumoral: peritumoral area, defined as 100 μm from the tumor boundary, Intratumoral: intratumoral area. $n=4$–5. **d** The phenotype of GAMs was analyzed by FACS on days 3, 7, 14, and 21 after tumor inoculation ($n=4$–5). $^*P<0.05$, $^{**}P<0.01$, $^{***}P<0.001$

We found that anti-PD-1 treatment, when given 7 days after tumor inoculation, led to a significant increase in the frequency of T cells but did not affect the proportion of CD8$^+$ T, CD4$^+$ T, or Treg cells (Fig. 4a). Meanwhile, anti-PD-1 treatment did not affect the frequency of GAMs. Still, it significantly increased the MHC-II$^+$iNOS$^+$ M1-like cells in GAMs (Fig. 4b). It is noteworthy that T cells and GAMs did not show significant changes in infiltration

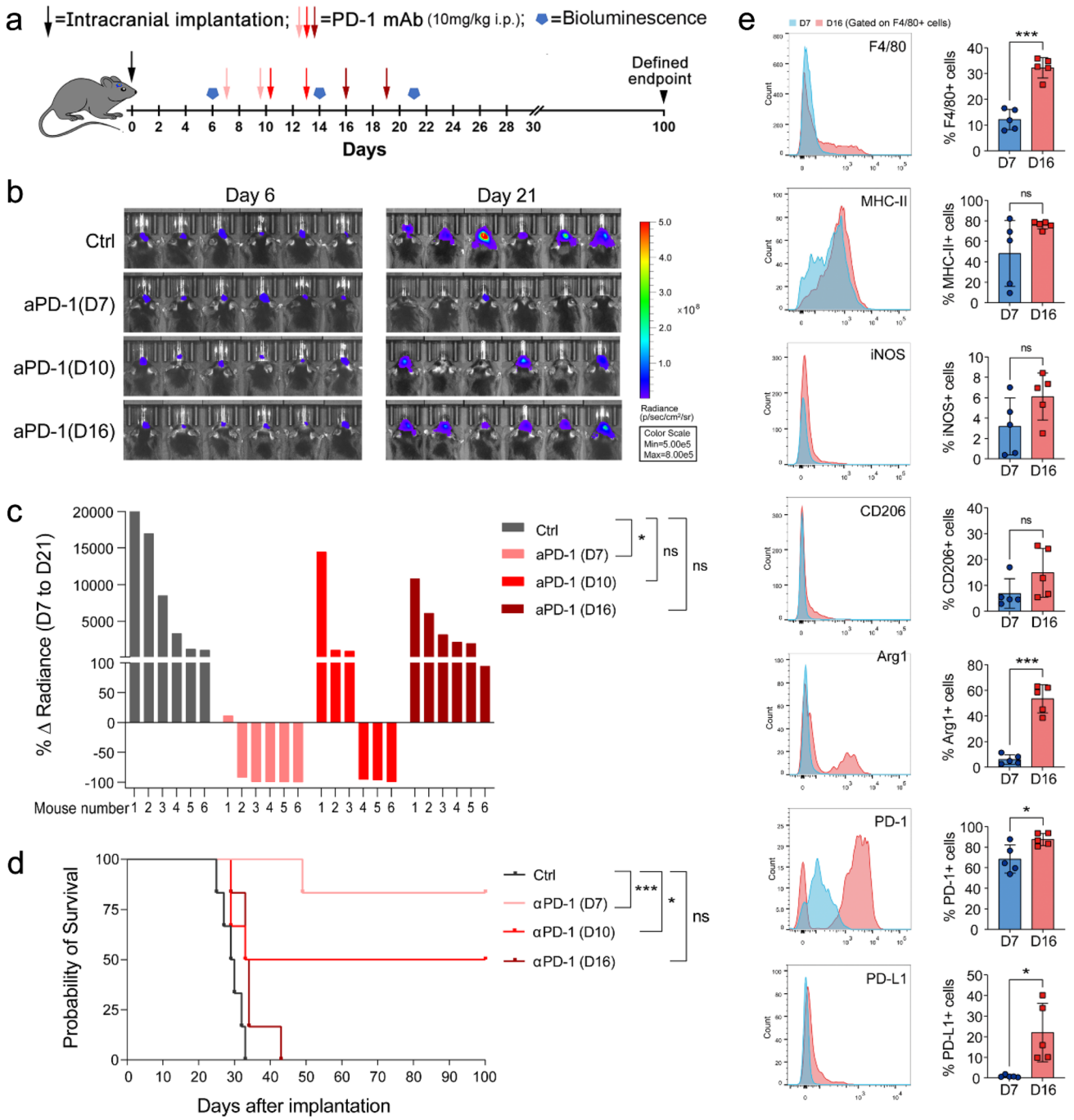

Fig. 2 Therapeutic effect of anti-PD-1 antibody and activation state of GAMs in glioma at different treatment times. **a** Experimental timeline. **b** Luciferase imaging of 6 distinct mice per treatment arm before and after treatment (days 6 and 21), divided by treatment group. All images were analyzed at the same color scale. **c** The waterfall plot showed the change in tumor volume on day 21 compared to day 6 for each mouse. **d** Kaplan–Meier survival curve showed a significant difference between the control and anti-PD-1 antibody arms. **e** Expression of immune molecules in GAMs on days 7 and 16 after tumor inoculation ($n=5$). $^{*}P<0.05$, $^{***}P<0.001$

or activation when anti-PD-1therapy began from day 16 postinoculation (data not shown). These results suggest that anti-PD-1 therapy can promote T cells infiltration and M1-like activation of GAMs, which are limited to early-stage tumors.

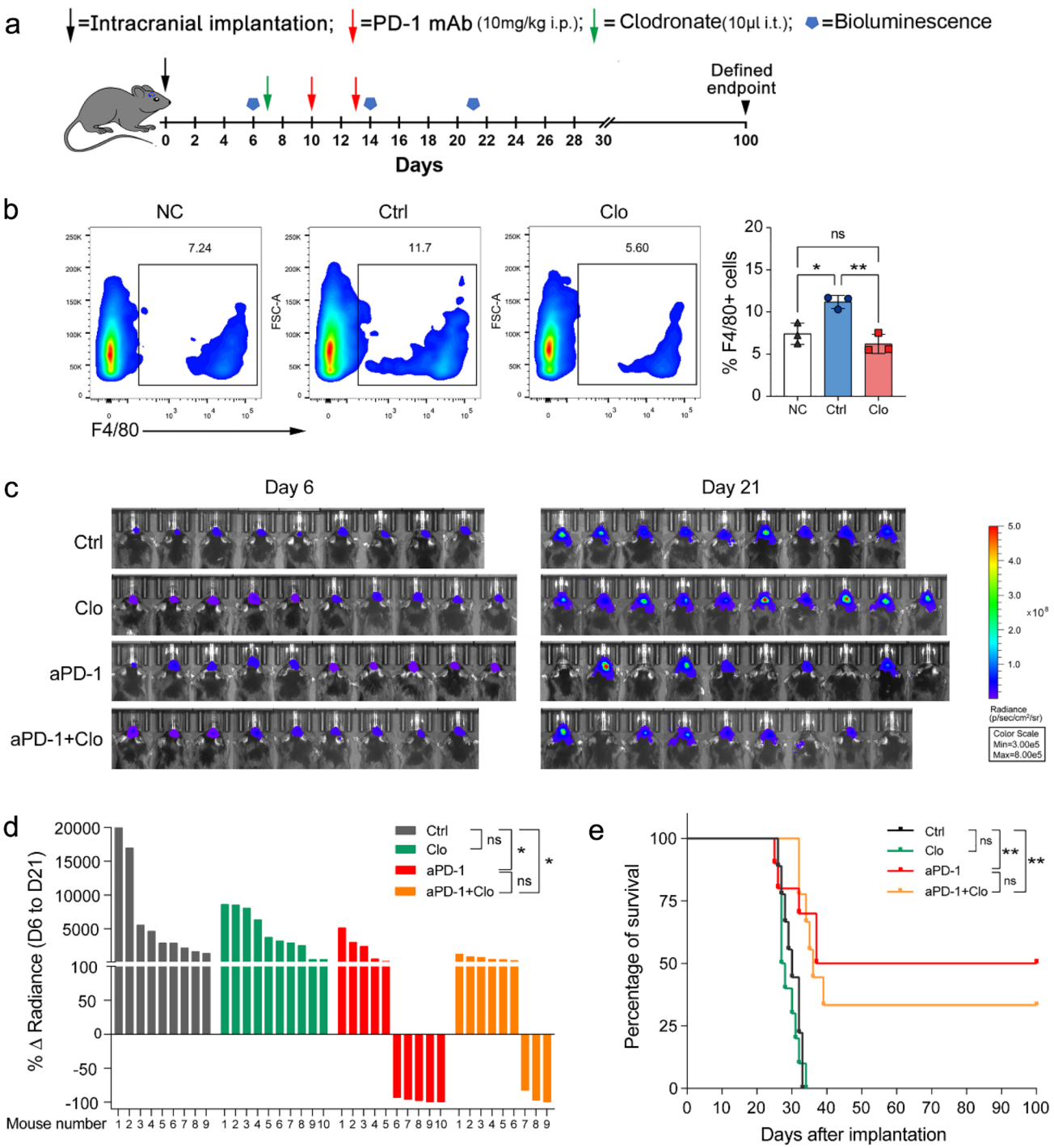

Fig. 3 Effect of GAMs depletion on anti-PD-1 therapy in glioma. **a** Experimental timeline (i.p., intraperitoneal injection, i.t., intratumoral injection). **b** F4/80^{+} cells proportion analysis five days after the clodronate liposome injection. (*NC* Normal brain control, *Clo* Clodronate, $n=3$). **c** Luciferase imaging of 9–10 distinct mice per treatment arm before and after treatment (days 6 and 21), divided by treatment group. All images were analyzed at the same color scale. **d** The waterfall plot showed the change in tumor volume on day 21 compared to day 6 for each mouse. **e** Kaplan–Meier survival curve. *$P<0.05$, **$P<0.01$

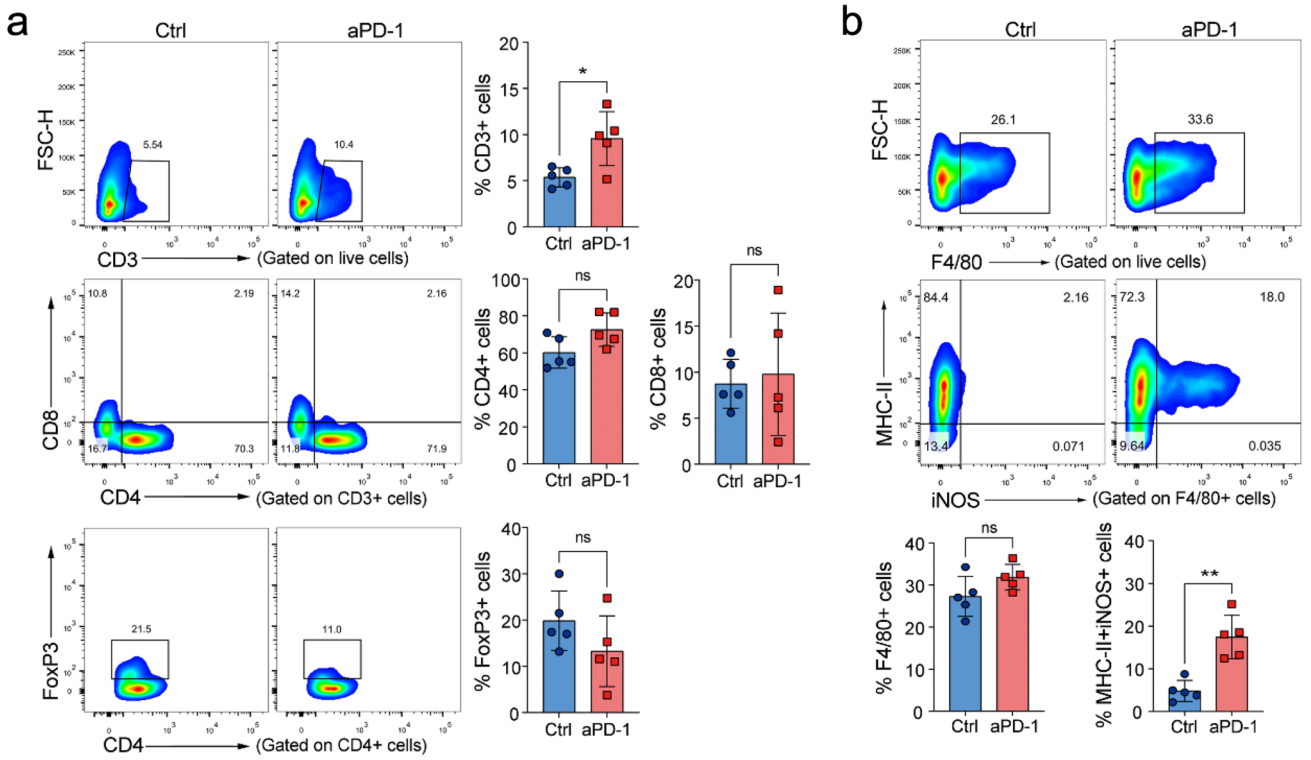

Fig. 4 Effect of anti-PD-1 therapy on tumor-infiltrating T cells and GAMs. After three days of anti-PD-1 antibody treatment began on day 7, the T cells and GAMs were analyzed by FACS. **a** Anti-PD-1 therapy promoted T cell infiltration but did not affect their proportion ($n=5$). **b** Anti-PD-1 therapy did not change the frequency of GAMs but increased MHC-II$^+$iNOS$^+$ M1-like cells ($n=5$). *$P<0.05$, **$P<0.01$, ***$P<0.001$

PD-L1 ablation reverses GAMs M2-like phenotypes and favors anti-PD-1 therapy

High levels of PD-L1 in cancer cells are associated with tumor immune evasion and response to anti-PD-1 therapy [28]. However, the role of GAMs-derived PD-L1 in anti-PD-1 therapy against gliomas remains unclear. We found that GAMs are the primary PD-L1-expressing non-neoplastic cells in the TME by FACS and immunofluorescence staining (Fig. 5a, b). To investigate the impact of GAMs-derived PD-L1 on anti-PD-1 therapy, we implanted wild-type GL261-Luc cells into PD-L1$^{-/-}$ mice. Our results showed that the lack of PD-L1 expression in host cells, mainly in GAMs, tended to prolong the survival time of tumor-bearing mice, although the difference did not reach statistical significance ($P=0.054$). Furthermore, a statistically nonsignificant trend in enhancing the efficacy of anti-PD-1 therapy was also observed in PD-L1$^{-/-}$ mice compared to WT mice (Fig. 5c–f). More importantly, PD-L1 deficiency markedly promoted the M1-like activation of GAMs, accompanied by upregulation of MHC-II, iNOS, CD80, CD86, and CD40 (Fig. 5g). These findings indicate that GAMs-derived PD-L1 is essential for maintaining M2-like activation of GAMs and modestly affects the efficacy of anti-PD-1 therapy.

Antigen-presenting ability impairment of GAMs limits CD4$^+$ T cell-mediated antitumor immunity in anti-PD-1 therapy

APCs, including microglia or macrophages, mediated MHC-II-restricted antigen presentation is essential for CD4$^+$ T cell-dependent antitumor immunity [29]. So we wondered whether GAMs might impact anti-PD-1 therapy through interaction with CD4$^+$ T cells. To explore this, we first confirmed the effect of CD4$^+$ T cells on anti-PD-1 therapy by depleting CD4$^+$ T cells. The results showed that CD4$^+$ T cell depletion promoted tumor outgrowth and eliminated anti-PD-1 efficacy in glioma-bearing mice (Fig. 6a–e). We also observed that CD4$^+$ T cells were in close contact with GAMs in the glioma microenvironment (Fig. 7a). Then we isolated primary microglia and co-cultured them with naïve CD4$^+$ T cells derived from OT-II mice (Extended Data Fig. 2a, b). We found that microglia loaded with OVA peptides could effectively induce the proliferation of naïve CD4$^+$ T cells, but proliferation was inhibited when microglia were preincubated with the tumor-conditioned medium (Fig. 7b). FACS analysis demonstrated

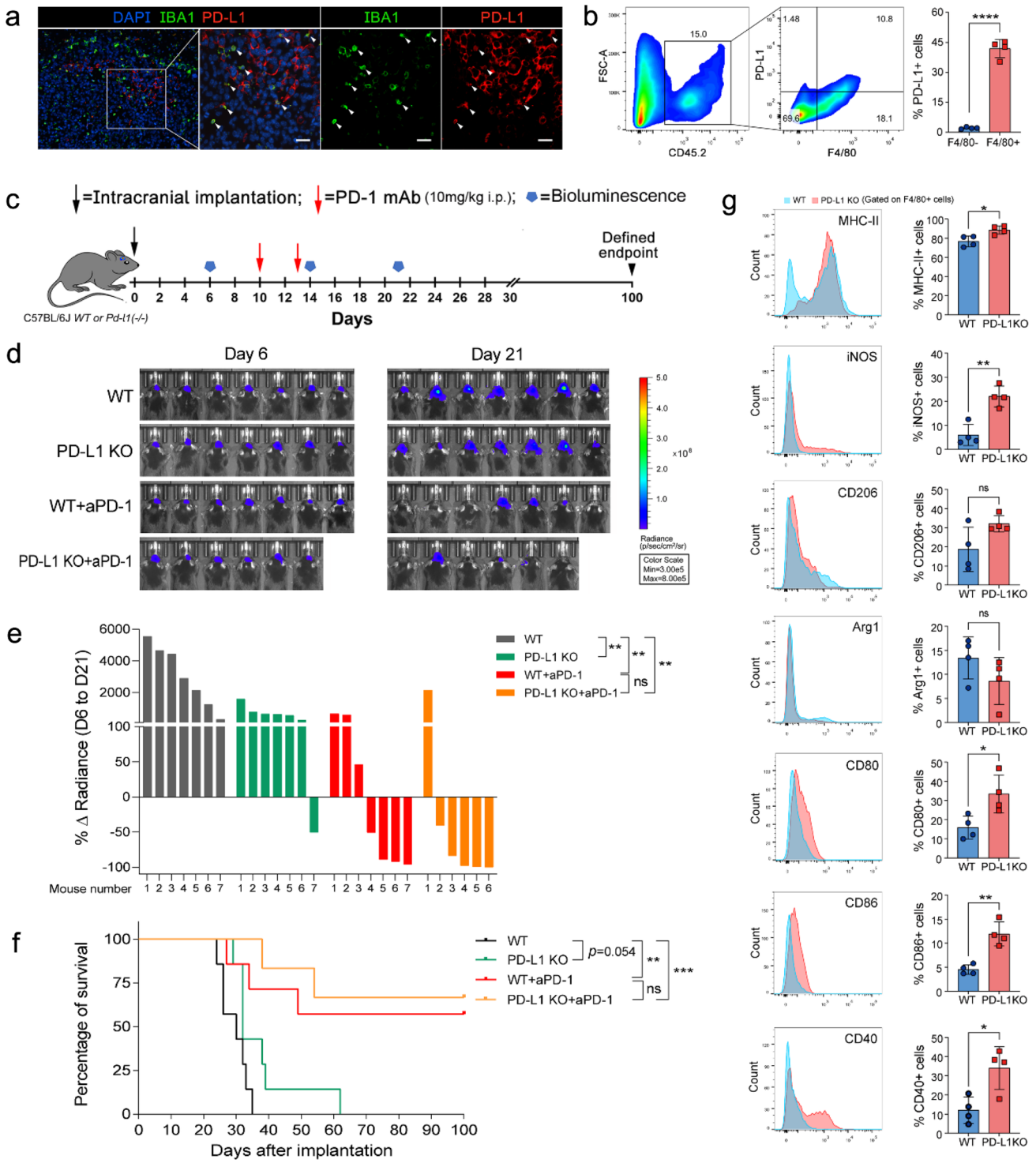

Fig. 5 Expression of PD-L1 in GAMs and the effect of PD-L1 knockout on GAMs activation and anti-PD-1 therapy. **a** Representative immunofluorescence staining for Iba1 (green), PD-L1 (red), and DAPI (blue) in glioma tissues. (scale: 50 μm) **b** Analysis of PD-L1 expression in GAMs ($CD45^+F4/80^+$) and non-GAMs immune cells ($CD45^+F4/80^-$) using FACS. **c** Experimental timeline. (i.p., intraperitoneal injection) **d** Luciferase imaging of 6–7 distinct mice per treatment arm before and after treatment (days 6 and 21), divided by treatment group. All images were analyzed at the same color scale. **e** The waterfall plot showed the change in tumor volume on day 21 compared to day 6 for each mouse ($n = 6 \sim 7$). **f** Kaplan–Meier survival curve ($n = 6 \sim 7$). **g** Analysis of GAMs activation in WT and PD-L1 KO glioma-bearing mice 14 days after tumor inoculation ($n = 4$). $^*P < 0.05$, $^{**}P < 0.01$, $^{***}P < 0.001$

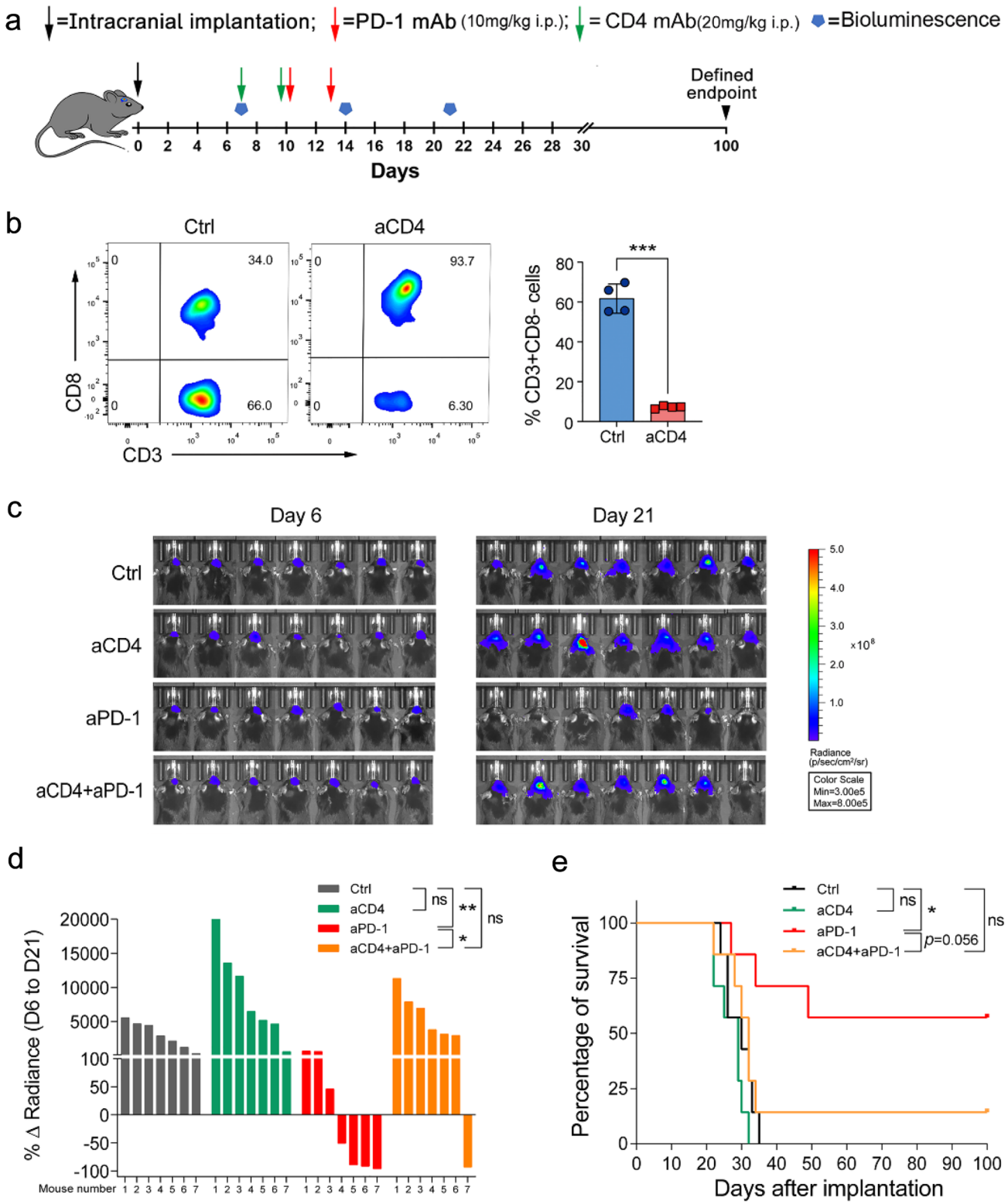

Fig. 6 Effect of $CD4^+$ T cells depletion on glioma anti-PD-1 therapy. **a** Experimental timeline (i.p., intraperitoneal injection). **b** Validation of $CD4^+$ T cells depletion three days after the last antibody injection by FACS ($n=4$). **c** Luciferase imaging of 7 distinct mice per treatment arm before and after treatment (days 6 and 21), divided by treatment group. All images were analyzed at the same color scale. **d** The waterfall plot showed the change in tumor volume on day 21 compared to day 6 for each mouse. **e** Kaplan–Meier survival curve. $^*P<0.05$, $^{***}P<0.001$

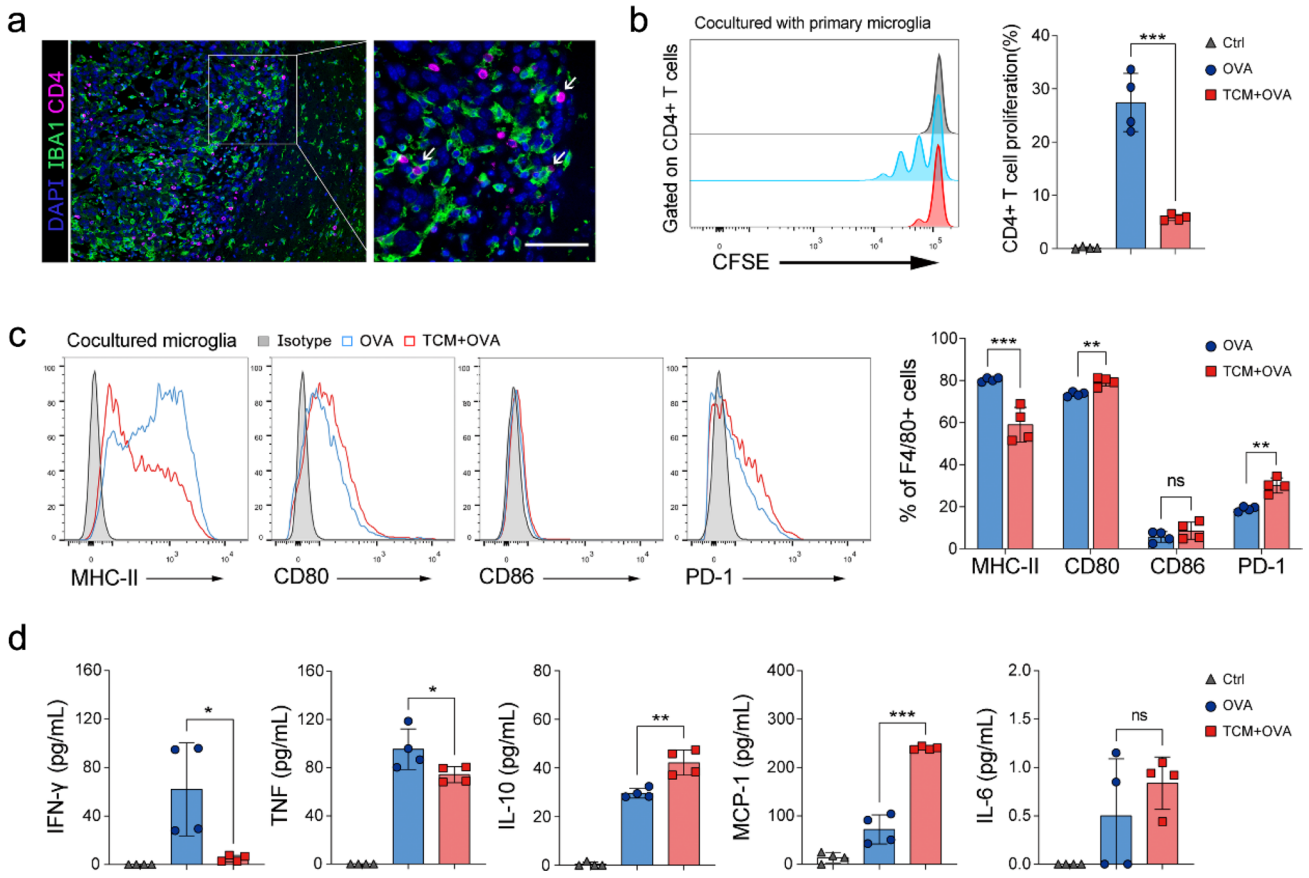

Fig. 7 Tumor-conditioned medium inhibits the proliferation and activation of $CD4^+$ T cells by impairing the antigen-presenting function of microglia. **a** Immunofluorescence staining shows that $CD4^+$ T cells (pink) contacted closely with GAMs (green) in the tumor microenvironment (scale: 50 μm). **b** The proliferation analysis of OT-II naïve $CD4^+$ T cells. After 72 h co-cultured with tumor-conditioned medium or DMEM pretreated OVA-loaded microglia, the proliferation of $CD4^+$ T cells was measured by flow cytometry based on CFSE signal ($n=4$). **c** Activation analysis of co-cultured microglia cells by FACS ($n=4$). **d** Detection of cytokines in co-cultured supernatant by cytometric bead array ($n=4$). *TCM* Tumor-conditioned medium, $^*P<0.05$, $^{**}P<0.01$, $^{***}P<0.001$

that tumor-conditioned medium treatment significantly downregulated MHC-II expression but upregulated CD80 and PD-1 expression in microglia (Fig. 7c). Moreover, cytokine analysis of co-cultured cell supernatants showed that tumor-conditioned medium treatment significantly decreased the expression of IFN-γ and TNF-α, but increased IL-10 and MCP-1 in microglia or $CD4^+$ T cells (Fig. 7d). These results suggest that tumor-induced downregulation of MHC-II expression in microglia could hinder antigen-specific $CD4^+$ T cell proliferation and Th1 differentiation, which may further impair the efficacy of anti-PD-1 therapy.

Discussion

In this study, we show that GAMs were able to adopt different phenotypes and affect the effect of anti-PD-1 immunotherapy on gliomas. At the early stage of the tumor, the application of anti-PD-1 is conducive to M1-like activation of GAMs and enhances the antitumor response. Correspondingly, the M2-like activation transition of GAMs in advanced tumors is difficult to reverse with anti-PD-1 therapy and is associated with therapy resistance. Furthermore, our experiments show that upregulation of PD-L1 or impairment of MHC-II expression inhibits the M1-like activation of GAMs.

Anti-PD-1 monotherapy for recurrent GBM patients has failed to show survival benefits [4, 30]. The mechanisms leading to therapy resistance are still poorly understood. Our results demonstrate that the efficacy of anti-PD-1 monotherapy in the GL261 model is closely related to the time of therapy initiation. Over 80% of GL261-bearing mice with long-term survival when given anti-PD-1 therapy 7 days after tumor inoculation, while no mice have survival benefits when given 16 days postinoculation (Fig. 2c, d). Whether tumor intrinsic or extrinsic factors constitute the main determinants of response and resistance to anti-PD-1 therapy is currently highly confusing [31]. Here, we show a potential association between GAMs activation and anti-PD-1 treatment response. The emergence of anti-PD-1 treatment resistance is accompanied by the transformation of GAMs from M1 to M2, which express more PD-1, PD-L1, and Arg1 (Fig. 2e). The initial state of GAMs has been reported to exhibit anti-glioblastoma activities and prolong the survival of PD-1-treated glioma-bearing mice, even when $CD8^+$ T cells are absent, which suggests that the innate immune system may mediate the therapeutic effects of anti-PD-1 [32, 33]. Here, we found that the depletion of GAMs could weaken the efficacy of anti-PD-1 therapy, supporting the above view (Fig. 3). Mechanistically, the anti-PD-1 therapy promotes M1-like activation in GAMs, which may contribute to the therapeutic efficacy (Fig. 4b). However, in advanced tumors, GAMs are hard to reprogram into M1-like phenotypes by anti-PD-1 therapy. All these results highlight the importance of the activation state of GAMs for the efficacy of anti-PD-1 therapy in gliomas.

High PD-L1 expression levels have been observed in tumor-associated APCs [34–36]. We confirmed that GAMs are the primary non-neoplastic cells that upregulate PD-L1 expression in gliomas (Figs. 1d, 5a, b). Importantly, we found that loss of PD-L1 expression on host cells, especially GAMs, markedly activated M1-like GAMs and could modestly improve anti-PD-1 therapy (Fig. 5d–g). PD-L1 has been found to provide backward signals restraining the antitumor activities of PD-L1-expressed T cells [37], so we reason PD-L1 also restricts the M1-like activation of GAMs. This inference also supports a recent report by Zhu et al., which shows that PD-L1 high expression in human GBM was significantly correlated with the M2-polarization of macrophages [17]. Our results highlight the role of the PD-1/PD-L1 pathway in GAMs M1/M2 activation and provide a new perspective to understand the underlying molecular and cellular mechanisms of PD-1/PD-L1 blockade therapy.

Accumulating evidence indicates the importance of $CD4^+$ T cells in tumor immunotherapy [26, 38, 39]. $CD4^+$ T cell depletion eliminated anti-PD-1 efficacy in our glioma-bearing mice model (Fig. 6c–e). $CD4^+$ T cell-mediated tumor rejection mainly depends on APCs that endocytose, process, and present tumor antigens on their MHC-II to activate tumor-specific $CD4^+$ T cells [40, 41]. Our results revealed that glioma-derived factors could impair MHC-II expression in microglia, the most critical APCs in the CNS [42], leading to the inhibition of antigen-specific proliferation and Th1 activation of $CD4^+$ T cells. In addition, a previous study showed that microglial MHC-II expression is downregulated in high-grade human gliomas [43]. These results further emphasize the impact of GAMs activation on anti-PD-1 therapy because of its potential effect on the antitumor immunity of $CD4^+$ T cells.

The major limitation of our study is that all the experiments were done with a single glioma model. GL261-Luc cells are known to be immunogenic and respond to anti-PD-1 therapy, which cannot accurately represent immunotherapy response in human GBM [44]. However, even though this model is PD-1-sensitive, PD-1 monotherapy does little to limit tumor progression when given 16 days postinoculation. These results suggest that the time when anti-PD-1 treatment can exert the best effect may be in the early-stage gliomas.

In summary, our study shows that GAMs can facilitate or hinder anti-PD-1 therapy depending on their activation state. M1-like GAMs are important for anti-PD-1 immunotherapy against glioma, while the accumulation of M2-like GAMs is associated with therapy resistance. Moreover, PD-L1 expression upregulated or MHC-II impaired in GAMs probably weakens anti-PD-1 therapy. These findings support GAMs as a potential biomarker for therapy response or target to improve anti-PD-1 treatment in gliomas.

Supplementary Information The online version contains supplementary material available at https://doi.org/10.1007/s00262-022-03358-3.

Acknowledgements We thank Cailing Yan at the Public Technology Service Center of Fujian Medical University for technical assistance with the bioluminescence imaging. This work was supported by the Natural Science Foundation of Fujian Province (No. 2019J01464) and the Joint Funds for the Innovation of Science and Technology, Fujian Province (No. 2018Y9053).

Author contributions CW and LL conceived and designed the experiments. CW and QC performed the experiments and collected and analyzed the data. MC cooperated with the establishment of tumor models. SG prepared the experimental materials and bred and identified gene knockout mice. PH and YZ isolated and purified the blocking antibodies. JW and BH provided technical guidance. CW wrote the first draft of the manuscript, and LL, QZ, and LC supervised the study and commented on previous versions of the manuscript. All authors have read and approved the final manuscript.

Data availability All data generated or analyzed in this study are included in this published article. Further details are available upon request.

Declarations

Conflict of interest The authors declare that they have no competing interests.

Ethical approval All procedures performed in studies involving animals were approved by the Fujian Medical University Institutional Animal Care and Use Committee (IACUC, No. 2019-0114) in accordance with ethical standards. All applicable international, national, and institutional guidelines for the care and use of animals were followed.

References

1. Miller KD, Ostrom QT, Kruchko C, Patil N, Tihan T, Cioffi G, Fuchs HE, Waite KA, Jemal A, Siegel RL, Barnholtz-Sloan JS (2021) Brain and other central nervous system tumor statistics, 2021. CA Cancer J Clin 71(5):381–406. https://doi.org/10.3322/caac.21693
2. Zou W, Wolchok JD, Chen L (2016) PD-L1 (B7–H1) and PD-1 pathway blockade for cancer therapy: mechanisms, response biomarkers, and combinations. Sci Transl Med 8(328):328rv324-328rv324. https://doi.org/10.1126/scitranslmed.aad7118
3. Ribas A, Wolchok JD (2018) Cancer immunotherapy using checkpoint blockade. Science (New York, N.Y.) 359(6382):1350–1355. https://doi.org/10.1126/science.aar4060
4. Reardon DA, Brandes AA, Omuro A, Mulholland P, Lim M, Wick A, Baehring J, Ahluwalia MS, Roth P, Bahr O, Phuphanich S, Sepulveda JM, De Souza P, Sahebjam S, Carleton M, Tatsuoka K, Taitt C, Zwirtes R, Sampson J, Weller M (2020) Effect of Nivolumab versus Bevacizumab in patients with recurrent glioblastoma: the checkmate 143 phase 3 randomized clinical trial. JAMA Oncol 6(7):1003–1010. https://doi.org/10.1001/jamaoncol.2020.1024
5. Wang X, Guo G, Guan H, Yu Y, Lu J, Yu J (2019) Challenges and potential of PD-1/PD-L1 checkpoint blockade immunotherapy for glioblastoma. J Exp Clin Cancer Res CR 38(1):87. https://doi.org/10.1186/s13046-019-1085-3
6. Lim M, Xia Y, Bettegowda C, Weller M (2018) Current state of immunotherapy for glioblastoma. Nat Rev Clin Oncol 15(7):422–442. https://doi.org/10.1038/s41571-018-0003-5
7. Woroniecka K, Chongsathidkiet P, Rhodin K, Kemeny H, Dechant C, Farber SH, Elsamadicy AA, Cui X, Koyama S, Jackson C, Hansen LJ, Johanns TM, Sanchez-Perez L, Chandramohan V, Yu YA, Bigner DD, Giles A, Healy P, Dranoff G, Weinhold KJ, Dunn GP, Fecci PE (2018) T-Cell exhaustion signatures vary with tumor type and are severe in Glioblastoma. Clin Cancer Res Off J Am Assoc Cancer Res 24(17):4175–4186. https://doi.org/10.1158/1078-0432.CCR-17-1846
8. Antonios JP, Soto H, Everson RG, Moughon D, Orpilla JR, Shin NP, Sedighim S, Treger J, Odesa S, Tucker A, Yong WH, Li G, Cloughesy TF, Liau LM, Prins RM (2017) Immunosuppressive tumor-infiltrating myeloid cells mediate adaptive immune resistance via a PD-1/PD-L1 mechanism in glioblastoma. Neuro Oncol 19(6):796–807. https://doi.org/10.1093/neuonc/now287
9. Nduom EK, Weller M, Heimberger AB (2015) Immunosuppressive mechanisms in glioblastoma. Neuro Oncol 17(7):9–14. https://doi.org/10.1093/neuonc/nov151
10. Charles NA, Holland EC, Gilbertson R, Glass R, Kettenmann H (2012) The brain tumor microenvironment. Glia 60(3):502–514. https://doi.org/10.1002/glia.21264
11. Hambardzumyan D, Gutmann DH, Kettenmann H (2016) The role of microglia and macrophages in glioma maintenance and progression. Nat Neurosci 19(1):20–27. https://doi.org/10.1038/nn.4185
12. Szulzewsky F, Pelz A, Feng X, Synowitz M, Markovic D, Langmann T, Holtman IR, Wang X, Eggen BJ, Boddeke HW, Hambardzumyan D, Wolf SA, Kettenmann H (2015) Glioma-associated microglia/macrophages display an expression profile different from M1 and M2 polarization and highly express Gpnmb and Spp1. PLoS ONE 10(2):e0116644. https://doi.org/10.1371/journal.pone.0116644
13. Li W, Graeber MB (2012) The molecular profile of microglia under the influence of glioma. Neuro Oncol 14(8):958–978. https://doi.org/10.1093/neuonc/nos116
14. Orihuela R, McPherson CA, Harry GJ (2016) Microglial M1/M2 polarization and metabolic states. Br J Pharmacol 173(4):649–665. https://doi.org/10.1111/bph.2016.173.issue-4
15. Yao A, Liu F, Chen K, Tang L, Liu L, Zhang K, Yu C, Bian G, Guo H, Zheng J, Cheng P, Ju G, Wang J (2014) Programmed death 1 deficiency induces the polarization of macrophages/microglia to the M1 phenotype after spinal cord injury in mice. Neurotherapeutics 11(3):636–650. https://doi.org/10.1007/s13311-013-0254-x
16. Roesch S, Rapp C, Dettling S, Herold-Mende C (2018) When immune cells turn bad-tumor-associated microglia/macrophages in Glioma. Int J Mol Sci 19(2):436. https://doi.org/10.3390/ijms19020436
17. Zhu Z, Zhang H, Chen B, Liu X, Zhang S, Zong Z, Gao M (2020) PD-L1-mediated immunosuppression in Glioblastoma is associated with the infiltration and M2-polarization of tumor-associated macrophages. Front Immunol 11:588552. https://doi.org/10.3389/fimmu.2020.588552
18. Miyauchi JT, Caponegro MD, Chen D, Choi MK, Li M, Tsirka SE (2018) Deletion of neuropilin 1 from microglia or bone marrow-derived macrophages slows glioma progression. Cancer Res 78(3):685–694. https://doi.org/10.1158/0008-5472.CAN-17-1435
19. Locarno CV, Simonelli M, Carenza C, Capucetti A, Stanzani E, Lorenzi E, Persico P, Della Bella S, Passoni L, Mavilio D, Bonecchi R, Locati M, Savino B (2019) Role of myeloid cells in the immunosuppressive microenvironment in gliomas. Immunobiology 225(1):151853. https://doi.org/10.1016/j.imbio.2019.10.002
20. Pinton L, Masetto E, Vettore M, Solito S, Magri S, D'Andolfi M, Del Bianco P, Lollo G, Benoit JP, Okada H, Diaz A, Della Puppa A, Mandruzzato S (2019) The immune suppressive microenvironment of human gliomas depends on the accumulation of bone marrow-derived macrophages in the center of the lesion. J Immunother Cancer 7(1):58. https://doi.org/10.1186/s40425-019-0536-x
21. Matias D, Balca-Silva J, da Graca GC, Wanjiru CM, Macharia LW, Nascimento CP, Roque NR, Coelho-Aguiar JM, Pereira CM, Dos Santos MF, Pessoa LS, Lima FRS, Schanaider A, Ferrer VP, Tania Cristina Leite de Sampaio e S, Moura-Neto V (2018) Microglia/astrocytes-glioblastoma crosstalk: crucial molecular mechanisms and microenvironmental factors. Front Cell Neurosci 12:235. https://doi.org/10.3389/fncel.2018.00235
22. Zhao J, Chen AX, Gartrell RD, Silverman AM, Aparicio L, Chu T, Bordbar D, Shan D, Samanamud J, Mahajan A, Filip I, Orenbuch R, Goetz M, Yamaguchi JT, Cloney M, Horbinski C, Lukas RV, Raizer J, Rae AI, Yuan J, Canoll P, Bruce JN, Saenger YM, Sims P, Iwamoto FM, Sonabend AM, Rabadan R (2019) Immune and genomic correlates of response to anti-PD-1 immunotherapy in glioblastoma. Nat Med 25(3):462–469. https://doi.org/10.1038/s41591-019-0349-y
23. Hutter G, Theruvath J, Graef CM, Zhang M, Schoen MK, Manz EM, Bennett ML, Olson A, Azad TD, Sinha R, Chan C, Assad Kahn S, Gholamin S, Wilson C, Grant G, He J, Weissman IL, Mitra SS, Cheshier SH (2019) Microglia are effector cells of CD47-SIRPalpha antiphagocytic axis disruption against glioblastoma. Proc Natl Acad Sci USA 116(3):997–1006. https://doi.org/10.1073/pnas.1721434116
24. Kennedy BC, Showers CR, Anderson DE, Anderson L, Canoll P, Bruce JN, Anderson RC (2013) Tumor-associated macrophages in glioma: friend or foe? J Oncol 2013:486912. https://doi.org/10.1155/2013/486912

25. Zuazo M, Arasanz H, Fernandez-Hinojal G, Garcia-Granda MJ, Gato M, Bocanegra A, Martinez M, Hernandez B, Teijeira L, Morilla I, Lecumberri MJ, Fernandez de Lascoiti A, Vera R, Kochan G, Escors D (2019) Functional systemic CD4 immunity is required for clinical responses to PD-L1/PD-1 blockade therapy. EMBO Mol Med 11(7):e10293. https://doi.org/10.15252/emmm.201910293
26. Alspach E, Lussier DM, Miceli AP, Kizhvatov I, DuPage M, Luoma AM, Meng W, Lichti CF, Esaulova E, Vomund AN, Runci D, Ward JP, Gubin MM, Medrano RFV, Arthur CD, White JM, Sheehan KCF, Chen A, Wucherpfennig KW, Jacks T, Unanue ER, Artyomov MN, Schreiber RD (2019) MHC-II neoantigens shape tumour immunity and response to immunotherapy. Nature 574(7780):696–701. https://doi.org/10.1038/s41586-019-1671-8
27. Dong H, Zhu G, Tamada K, Flies D, van Deursen J, Chen L (2004) B7–H1 determines accumulation and deletion of intrahepatic CD8(+) T lymphocytes. Immunity 20(3):327–336. https://doi.org/10.1016/s1074-7613(04)00050-0
28. Lu S, Stein JE, Rimm DL, Wang DW, Bell JM, Johnson DB, Sosman JA, Schalper KA, Anders RA, Wang H, Hoyt C, Pardoll DM, Danilova L, Taube JM (2019) Comparison of biomarker modalities for predicting response to PD-1/PD-L1 checkpoint blockade: a systematic review and meta-analysis. JAMA Oncol 5(8):1195–1204. https://doi.org/10.1001/jamaoncol.2019.1549
29. Haabeth OAW, Fauskanger M, Manzke M, Lundin KU, Corthay A, Bogen B, Tveita AA (2018) CD4(+) T-cell-mediated rejection of MHC class II-positive tumor cells is dependent on antigen secretion and indirect presentation on host APCs. Cancer Res 78(16):4573–4585. https://doi.org/10.1158/0008-5472.CAN-17-2426
30. de Groot J, Penas-Prado M, Alfaro-Munoz KD, Hunter K, Pei B, O'Brien B, Weathers SP, Loghin M, Kamiya Matsouka C, Yung WKA, Mandel J, Wu J, Yuan Y, Zhou S, Fuller GN, Huse J, Rao G, Weinberg JS, Prabhu SS, McCutcheon IE, Lang FF, Ferguson SD, Sawaya R, Colen R, Yadav SS, Blando J, Vence L, Allison J, Sharma P, Heimberger AB (2019) Window-of-opportunity clinical trial of pembrolizumab in patients with recurrent glioblastoma reveals predominance of immune-suppressive macrophages. Neuro Oncol 22(4):539–549. https://doi.org/10.1093/neuonc/noz185
31. Chocarro de Erauso L, Zuazo M, Arasanz H, Bocanegra A, Hernandez C, Fernandez G, Garcia-Granda MJ, Blanco E, Vera R, Kochan G, Escors D (2020) Resistance to PD-L1/PD-1 Blockade Immunotherapy. A tumor-intrinsic or tumor-extrinsic phenomenon? Front Pharmacol 11:441. https://doi.org/10.3389/fphar.2020.00441
32. Sarkar S, Döring A, Zemp FJ, Silva C, Lun X, Wang X, Kelly J, Hader W, Hamilton M, Mercier P, Dunn JF, Kinniburgh D, van Rooijen N, Robbins S, Forsyth P, Cairncross G, Weiss S, Yong VW (2013) Therapeutic activation of macrophages and microglia to suppress brain tumor-initiating cells. Nat Neurosci 17(1):46–55. https://doi.org/10.1038/nn.3597
33. Rao G, Latha K, Ott M, Sabbagh A, Marisetty A, Ling X, Zamler D, Doucette TA, Yang Y, Kong LY, Wei J, Fuller GN, Benavides F, Sonabend AM, Long J, Li S, Curran M, Heimberger AB (2020) Anti-PD-1 induces M1 polarization in the glioma microenvironment and exerts therapeutic efficacy in the absence of CD8 cytotoxic T cells. Clin Cancer Res Off J Am Assoc Cancer Res 26(17):4699–4712. https://doi.org/10.1158/1078-0432.CCR-19-4110
34. Lin H, Wei S, Hurt EM, Green MD, Zhao L, Vatan L, Szeliga W, Herbst R, Harms PW, Fecher LA, Vats P, Chinnaiyan AM, Lao CD, Lawrence TS, Wicha M, Hamanishi J, Mandai M, Kryczek I, Zou W (2018) Host expression of PD-L1 determines efficacy of PD-L1 pathway blockade-mediated tumor regression. J Clin Investig 128(2):805–815. https://doi.org/10.1172/JCI96113
35. Bloch O, Crane CA, Kaur R, Safaee M, Rutkowski MJ, Parsa AT (2013) Gliomas promote immunosuppression through Induction of B7–H1 expression in tumor-associated macrophages. Clin Cancer Res 19(12):3165–3175. https://doi.org/10.1158/1078-0432.ccr-12-3314
36. Curiel TJ, Wei S, Dong H, Alvarez X, Cheng P, Mottram P, Krzysiek R, Knutson KL, Daniel B, Zimmermann MC, David O, Burow M, Gordon A, Dhurandhar N, Myers L, Berggren R, Hemminki A, Alvarez RD, Emilie D, Curiel DT, Chen L, Zou W (2003) Blockade of B7–H1 improves myeloid dendritic cell-mediated antitumor immunity. Nat Med 9(5):562–567. https://doi.org/10.1038/nm863
37. Diskin B, Adam S, Cassini MF, Sanchez G, Liria M, Aykut B, Buttar C, Li E, Sundberg B, Salas RD, Chen R, Wang J, Kim M, Farooq MS, Nguy S, Fedele C, Tang KH, Chen T, Wang W, Hundeyin M, Rossi JAK, Kurz E, Haq MIU, Karlen J, Kruger E, Sekendiz Z, Wu D, Shadaloey SAA, Baptiste G, Werba G, Selvaraj S, Loomis C, Wong KK, Leinwand J, Miller G (2020) PD-L1 engagement on T cells promotes self-tolerance and suppression of neighboring macrophages and effector T cells in cancer. Nat Immunol 21(4):442–454. https://doi.org/10.1038/s41590-020-0620-x
38. Tran E, Turcotte S, Gros A, Robbins PF, Lu YC, Dudley ME, Wunderlich JR, Somerville RP, Hogan K, Hinrichs CS, Parkhurst MR, Yang JC, Rosenberg SA (2014) Cancer immunotherapy based on mutation-specific CD4+ T cells in a patient with epithelial cancer. Science (New York, N.Y.) 344(6184):641–645. https://doi.org/10.1126/science.1251102
39. Kreiter S, Vormehr M, van de Roemer N, Diken M, Lower M, Diekmann J, Boegel S, Schrors B, Vascotto F, Castle JC, Tadmor AD, Schoenberger SP, Huber C, Tureci O, Sahin U (2015) Mutant MHC class II epitopes drive therapeutic immune responses to cancer. Nature 520(7549):692–696. https://doi.org/10.1038/nature14426
40. Haabeth OA, Tveita AA, Fauskanger M, Schjesvold F, Lorvik KB, Hofgaard PO, Omholt H, Munthe LA, Dembic Z, Corthay A, Bogen B (2014) How Do CD4(+) T cells detect and eliminate tumor cells that either lack or express MHC class II molecules? Front Immunol 5:174. https://doi.org/10.3389/fimmu.2014.00174
41. Corthay A, Skovseth DK, Lundin KU, Rosjo E, Omholt H, Hofgaard PO, Haraldsen G, Bogen B (2005) Primary antitumor immune response mediated by CD4+ T cells. Immunity 22(3):371–383. https://doi.org/10.1016/j.immuni.2005.02.003
42. Ulvestad E, Williams K, Bjerkvig R, Tiekotter K, Antel J, Matre R (1994) Human microglial cells have phenotypic and functional characteristics in common with both macrophages and dendritic antigen-presenting cells. J Leukoc Biol 56(6):732–740. https://doi.org/10.1002/jlb.56.6.732
43. Tran C, Wolz P, Egensperger R, Kösel S, Imai Y, Bise K, Kohsaka S, Mehraein P, Graeber M (1998) Differential expression of MHC class II molecules by microglia and neoplastic astroglia: relevance for the escape of astrocytoma cells from immune surveillance. Neuropathol Appl Neurobiol 244(4):293–301. https://doi.org/10.1046/j.1365-2990.1998.00120.x
44. Tritz ZP, Ayasoufi K, Johnson AJ (2021) Anti-PD-1 checkpoint blockade monotherapy in the orthotopic GL261 glioma model: the devil is in the detail. Neuro-Oncol Adv 3(1):1–9. https://doi.org/10.1093/noajnl/vdab066